Accepted Manuscript

Synthesis and evaluation of 4-hydroxyl aurone derivatives as multifunctional agents for the treatment of Alzheimer's disease

Yan Li, Xiaoming Qiang, Li Luo, Yuxing Li, Ganyuan Xiao, Zhenghuai Tan, Yong Deng

PII: S0968-0896(16)30246-2
DOI: http://dx.doi.org/10.1016/j.bmc.2016.04.012
Reference: BMC 12926

To appear in: *Bioorganic & Medicinal Chemistry*

Received Date: 10 March 2016
Revised Date: 5 April 2016
Accepted Date: 5 April 2016

Please cite this article as: Li, Y., Qiang, X., Luo, L., Li, Y., Xiao, G., Tan, Z., Deng, Y., Synthesis and evaluation of 4-hydroxyl aurone derivatives as multifunctional agents for the treatment of Alzheimer's disease, *Bioorganic & Medicinal Chemistry* (2016), doi: http://dx.doi.org/10.1016/j.bmc.2016.04.012

Synthesis and evaluation of 4-hydroxyl aurone derivatives as multifunctional agents for the treatment of Alzheimer's disease

Yan Li[a], Xiaoming Qiang[a], Li Luo[a], Yuxing Li[a], Ganyuan Xiao[a], Zhenghuai Tan[b,*], Yong Deng[a,*]

[a]*Department of Medicinal Chemistry, Key Laboratory of Drug Targeting and Drug Delivery System of the Education Ministry, West China School of Pharmacy, Sichuan University, Chengdu, 610041, China*

[b]*Institute of Traditional Chinese Medicine Pharmacology and Toxicology, Sichuan academy of Chinese Medicine Sciences, Chengdu, 610041, China*

**Corresponding Author*.

Phone, +86-28-85258982; E-mail: tanzhh616@163.com (Zhenghuai Tan)

Phone, +86-28-85503790; E-mail: dengyong@scu.edu.cn (Yong Deng)

Abstract

A series of 4-hydroxyl aurone derivatives were designed synthesized and evaluated as potential multifunctional agents for the treatment of Alzheimer's disease. The results demonstrated that most of the derivatives exhibited good multifunctional properties. Among them, compound **14e** displayed good inhibitory activities of self- and Cu^{2+}-induced A$\beta_{1\text{-}42}$ aggregation with 99.2% and 84.0% at 25 μM respectively, and high antioxidant activity with a value 1.90-fold of Trolox. In addition, **14e** also showed remarkable inhibitory activities of both monoamine oxidase A and B with IC_{50} values of 0.271 μM and 0.393 μM respectively. However the 6-methoxyl aurones **15a-c** revealed excellent selectivity toward MAO-B. Furthermore, the representative compounds **14e** and **15b** displayed good metal-chelating abilities and blood-brain barrier (BBB) permeabilities *in vitro*.

Keywords:

Alzheimer's disease; aurone derivatives; multifunctional agents; *β*-amyloid aggregation; monoamine oxidase.

1. Introduction

Alzheimer's disease (AD), an age-related neurodegenerative disorder of the central nervous system (CNS), is characterized by insidious onset of memory loss, progressive cognitive deterioration, impairment of activities of daily living and loss of independent function.[1] In addition, 50-80% of AD patients suffer from behavioral and psychological symptoms such as depression, psychosis and agitation.[2] Although the etiology of AD remains elusive, multiple factors such as β-amyloid (Aβ) deposits, τ-protein aggregation, oxidative stress, dyshomeostasis of biometals and decreased levels of acetylcholine (ACh) are considered to play vital roles in the pathophysiology of AD.[3] According to the amyloid cascade hypothesis, the increased production and accumulation of Aβ oligomeric aggregates in the brain are considered as a central event in the pathogenesis of AD, initiating the pathogenic cascade and ultimately leading to neuronal loss and dementia.[4] The $A\beta_{1\text{-}40}$ and $A\beta_{1\text{-}42}$ are the major isoforms of Aβ peptides. $A\beta_{1\text{-}40}$ is expressed in larger amounts in the brain, yet $A\beta_{1\text{-}42}$ displays lower solubility and more neurotoxic and has a higher tendency to aggregate.[5,6] Therefore, preventing the $A\beta_{1\text{-}42}$ aggregation is a potent therapeutic strategy for AD treatment.

In addition, the dyshomeostasis of metal ions such as Cu^{2+}, Fe^{2+}, Zn^{2+} and Al^{3+} clearly occurs in AD brains.[7] Studies suggest that excess of these metal ions have been found in Aβ plaques and they are closely associated with the formation of Aβ plaques and neurofibrillary tangles.[8] Moreover, the abnormally high levels of these redox-active metals could promote the production of reactive oxygen species (ROS) and oxidative stress.[9] However, oxidative stress is one of the earliest events in the pathogenesis of AD and may occur before the onset of memory loss, the appearance of senile plaques and neurofibrillary tangles.[10] And oxidative damage plays a crucial role in neuronal degeneration, which can harm biological molecules such as proteins, DNA, and lipids.[11,12] It is demonstrated that Aβ catalyses the reduction of Cu^{2+} and Fe^{3+}, which could lead to the production of ROS. In turn, oxidative stress may promote Aβ accumulation by generating the modified Aβ species which are prone to aggregate and resistant to clearance.[13] Thus, biometals chelators and antioxidants have been proposed as potential therapeutic agents against AD.

Monoamine oxidase A and B (MAO-A and -B) are flavin adenine dinucleotide (FAD)-containing enzymes, bound to the membrane surface of mitochondria and involved in the degradation of neurotransmitters and xenobiotic amines. These enzymes are responsible for

regulation and metabolism of major monoamine neurotransmitters such as serotonin, dopamine and noradrenaline.[14] Selective MAO-A inhibitors are used in clinical practice for the treatment of depression and anxiety, while MAO-B inhibitors are used to slow down the progression of Parkinson's disease (PD) and symptoms associated with AD. However, the biochemical activity of MAO generates hydroxyl radicals, which are harmful members of the oxygen free radical group involved in many neurodegenerative disorders like AD.[15] Recently, MAO inhibitors have been re-evaluated as potential therapeutics against many age-related pathologies, for example AD and PD. And in these diseases, neurotoxicity, protein misfolding and/or aggregation, iron accumulation, mitochondrial damage, and oxidative stress have been considered as major downstream causes.[16,17] As mentioned above, MAO could be a potential therapeutic target of AD and other psychiatric and neurological diseases. In fact, selective MAO-B inhibitors such as selegiline and rasagiline are beneficial for the treatment of PD and AD, and selective MAO-A inhibitors such as clorgyline and moclobemide are useful for the treatment of neurological disorders, for example depression and anxiety.[15]

Because of the complicated and multifactorial etiology, the "one-molecule, one-target" paradigm seems not so effective in treating complex diseases like AD. It can only improve clinical symptoms but cannot mitigate progression of the disease. Therefore, with the development of multi-target-directed ligands (MTDLs), it is significant to develop novel multifunctional drugs with two or more complementary bioactivities for the treatment of complex diseases as AD.[18-20]

Aurones, 2-benzylidenebenzofuran-3(2*H*)-ones, which are structural isomerides of flavones, are present in vegetables and flowers (**Figure 1**, **1**).[21] Aurones have attracted considerable attentions in recent years because they possess a wide range of bioactivities associated with neurological diseases especially for AD. Many studies have shown that naturally occurring aurones as well as the chemically synthesized analogs exhibited high affinities toward Aβ aggregates[22-24] and good MAO inhibitory activities[25,26]. These results suggest that aurone could be an excellent leading scaffold to design multifunctional drugs against AD. Recently, Masahiro Ono *et al.* reported an aurone analog, which possess a radioiodine at 5-position and a dimethylamino group 4'-position (**Figure 1**, **2**). It could serve as a probe of Aβ plaques in AD, with high binding affinity (K_i = 6.82 nM).[23] In addition, some studies have shown that electron-donating groups like dimethylamino group are closely associated with the binding affinity to Aβ aggregates.[27] Collectively, we designed a series of aurone

derivatives that are expected to be multifunctional agents with anti-Aβ aggregation, MAO inhibition, antioxidant and biometal chelating properties (**Figure 2**). Our derivatives reported in this study are either novel compounds, or although known substances[28-31] their testing as multifunctional anti-AD agents has not been reported.

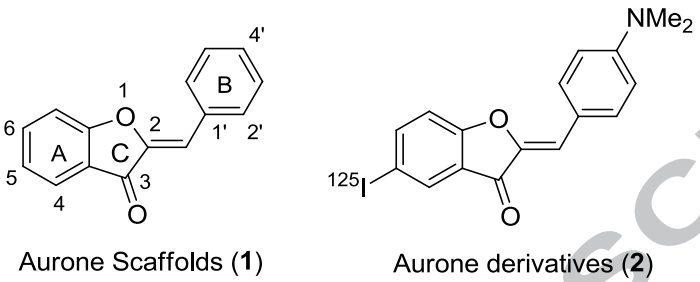

Figure 1. Aurone scaffolds (**1**) and aurone derivative (**2**) as Aβ plaques probes.

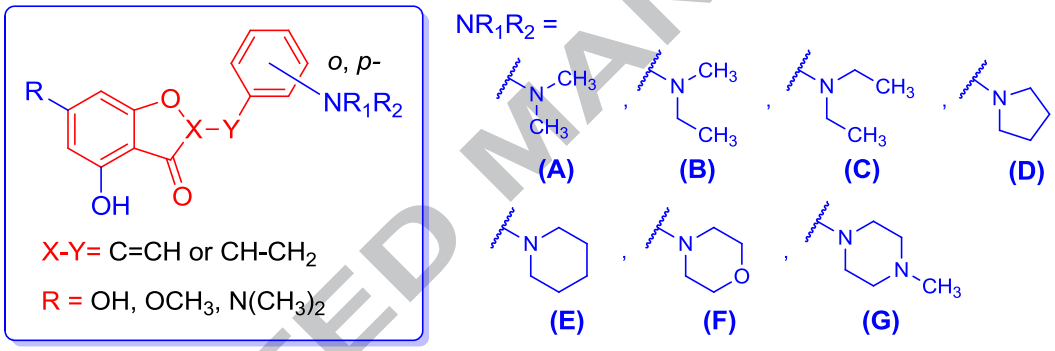

Figure 2. Structures of the designed multifunctional aurone derivatives **14-17**.

2. Results and discussion

2.1. Chemistry

The synthetic pathways of target derivatives were summarized in **Scheme 1** and **2**. Substituted benzaldehydes **8b-h** were synthesized according to well-established method.[32] The key intermediate **5** was produced from phloroglucinol **3** after Fries rearrangement and cyclization reaction. Compound **7** was obtained by the dimethylation of **5** and subsequent selective deprotection due to the difficulty of direct transformation from **5** to **7**.[33] Target compounds **14a-h** and **15a-c** were afforded by the condensation of **5** or **7** with corresponding substituted benzaldehydes **8a-h** in ethanolic 50% KOH solution. As reported in many literatures, only *Z* stereoisomers were isolated. The stereochemistry of the aurone diastereomers has been elucidated by NMR spectroscopic measurements and by X-ray diffraction analysis.[29,34-36] Compound **16a** and **16b** were obtained through catalytic hydrogenation of

14a and **14f** with 10% Pd/C as catalyst in THF. The synthesis of **11** was reported by our group previously.[6] The condensation of **11** with *p*-dimethylaminobenzaldehyde (**8a**) in ethanolic 50% KOH solution afforded chalcone **12**. Subsequently, cyclization of **12** with mercuric acetate in pyridine produced compound **13**, deprotection of which afforded the target compound **17**. All the aurone derivatives were characterized by ^{1}H NMR and HR-ESI-MS, and parts of them were further characterized by ^{13}C NMR.

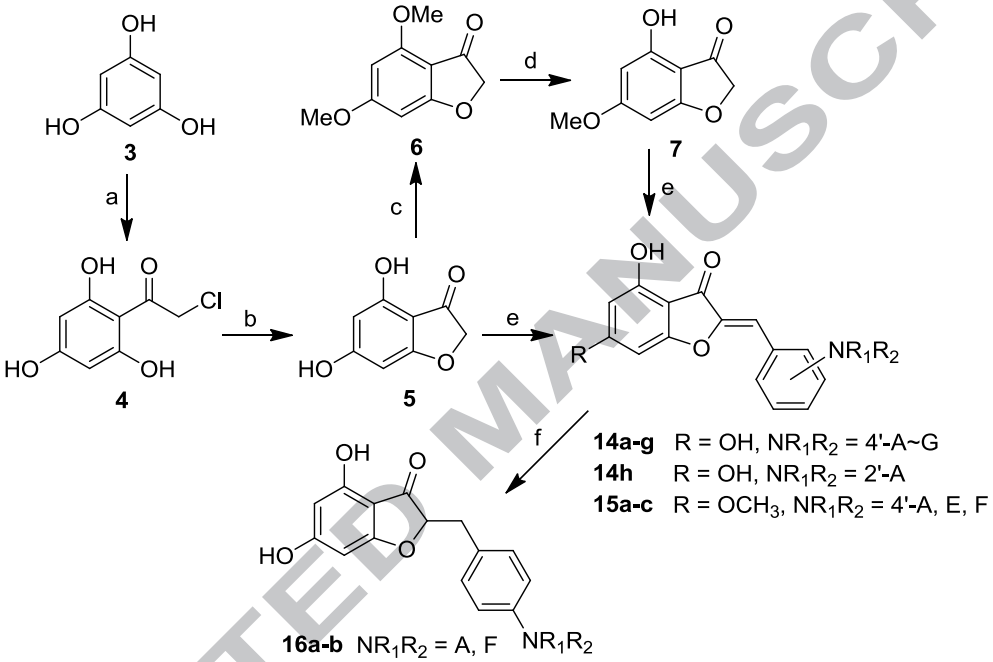

Scheme 1. Synthesis of aurone derivatives **14-16**. *Reagents and conditions:* (a) $ClCH_2COCl$, $AlCl_3$, EtOAc, r.t., overnight; then 50 °C, 6 h; (b) NaOAc, MeOH, reflux for 4 h; (c) Me_2SO_4, K_2CO_3, dimethoxyethane, reflux for 5 h; (d) $AlCl_3$, CH_2Cl_2, reflux for 5 h; (e) 2- or 4-substituted benzaldehyde (**8a-h**), 50% KOH, EtOH, r.t., overnight; (f) H_2, 10% Pd/C, THF, r.t., overnight.

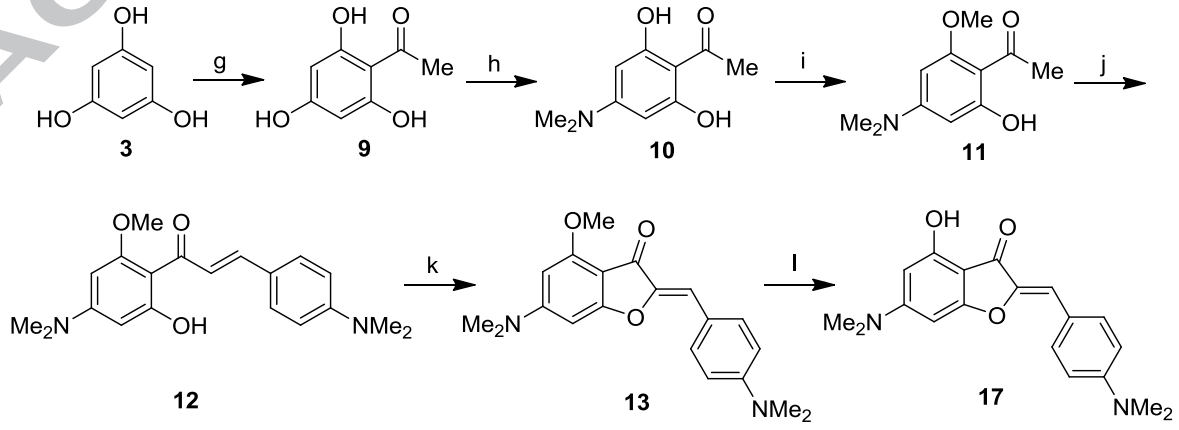

Scheme 2. Synthesis of aurone derivatives **17**. *Reagents and conditions:* (g) Ac_2O, BF_3•Et_2O, EtOAc,

50 °C, 10 h; (h) $HN(CH_3)_2$•HCl, $NaHCO_3$, H_2O, 70 °C, 10 h; (i) Me_2SO_4, K_2CO_3, acetone, reflux for 5 h; (j) (4-Me_2N)benzaldehyde (**8a**), 50% KOH, EtOH, r.t., overnight; (k) $Hg(OAc)_2$, pyridine, reflux for 15 h; (l) 40% HBr, 100 °C, 2 h.

2.2. Pharmacology

2.2.1. Inhibition of self- and Cu^{2+}-induced Aβ_{1-42} aggregation

The inhibition of self- and Cu^{2+}-induced Aβ_{1-42} aggregation by our synthetic derivatives was determined by using thioflavin T (ThT) assay, with curcumin as a reference compound.[37,38] The results summarized in **Table 1** indicated that these aurone derivatives exhibited moderate to good inhibitory activities of self- and Cu^{2+}-induced Aβ_{1-42} aggregation (22.3-99.8% and 20.9-90.1% at 25 μM respectively) compared with that of curcumin (41.3 ± 0.9% and 67.2 ± 1.3% respectively). Noticeably, the potencies of dihydroxy aurones **14a-h** were much higher than those of corresponding monohydroxy aurones and the reduction products. It revealed that 6-hydroxy group in aurone may strengthen the interaction between the derivatives and Aβ_{1-42} protein and the α, β-unsaturated ketone skeleton of aurone was essential for the potency. From the comparison between the potencies of **14a** and **14h**, we could find that the substitution position of amino groups may have no obvious impact on the inhibitory activities of Aβ_{1-42} aggregation. The results of **14a-h** demonstrated that, unlike hydroxyl group, diverse amino groups showed no significant difference between the effects on potencies (except for **14f** and **14g)**. Compared the potencies of **14a** and **17**, we could find that the transformation of 6-OH to 6-$N(CH_3)_2$ lowered the inhibitory activity, further indicating the importance of 6-OH group.

Table 1. In vitro inhibition of self- and Cu^{2+}-induced Aβ_{1-42} aggregation, MAO inhibitory activities and oxygen radical absorbance capacity (ORAC, Trolox equivalents) of aurone derivatives and reference compounds.

Compd.	%Inhibition of Aβ_{1-42} aggregation[a]		IC_{50} ± SD (μM)		SI[e]	ORAC[f,g]
	Self-induced[b,g]	Cu^{2+}-induced[c,g]	MAO-A[d,g]	MAO-B[d,g]		
14a	97.4 ± 1.3	61.4 ± 2.2	0.233 ± 0.005	5.940 ± 0.021	0.039	2.90 ± 0.03
14b	95.3 ± 2.0	86.6 ± 1.7	0.0279 ± 0.004	0.808 ± 0.023	0.035	1.97 ± 0.07
14c	91.7 ± 2.1	88.9 ± 3.1	0.115 ± 0.009	0.334 ± 0.008	0.344	2.04 ± 0.05
14d	99.8 ± 1.5	84.8 ± 1.6	0.457 ± 0.010	0.391 ± 0.011	1.169	1.56 ± 0.02
14e	99.2 ± 1.1	84.0 ± 1.5	0.271 ± 0.013	0.393 ± 0.025	0.690	1.90 ± 0.09
14f	80.7 ± 1.7	50.1 ± 3.1	1.08 ± 0.024	0.34 ± 0.031	3.176	2.50 ± 0.05
14g	77.7 ± 2.4	52.0 ± 2.8	15.8% ± 0.9%	10.8 ± 0.102	> 0.926	2.50 ± 0.05

14h	98.2 ± 1.6	90.1 ± 1.3	13.5% ± 1.0%	0.88% ± 0.3%	—	2.91 ± 0.02
15a	53.7 ± 1.3	75.7 ± 1.2	20.7% ± 1.5%	0.703 ± 0.043	> 14.225	1.62 ± 0.08
15b	40.3 ± 1.0	46.0 ± 1.9	18.3% ± 1.1%	0.226 ± 0.017	> 44.248	1.00 ± 0.06
15c	44.1 ± 2.1	47.5 ± 2.2	18.4% ± 1.4%	1.50 ± 0.098	> 6.667	1.66 ± 0.04
16a	42.7 ± 2.2	40.5 ± 2.6	23.5% ± 2.5%	27.2% ± 2.9%	—	3.07 ± 0.17
16b	38.0 ± 2.4	20.9 ± 2.1	13.9% ± 1.2%	8.7% ± 1.0%	—	3.56 ± 0.14
17	22.3 ± 1.2	71.6 ± 1.3	16.8% ± 2.1%	13.5% ± 1.2%	—	2.43 ± 0.12
Curcumin	41.3 ± 0.9	67.2 ± 1.3	—	—	—	—
Clorgyline	—	—	0.0027 ± 0.0006	4.19 ± 0.101	0.00064	—
Rasagiline	—	—	1.42 ± 0.015	0.0825 ± 0.002	17.21	—
Iproniazid	—	—	2.56 ± 0.023	1.95 ± 0.074	1.31	—

[a] For inhibition of Aβ aggregation, the thioflavin-T fluorescence method was used.

[b] Inhibition of self-induced A$\beta_{1\text{-}42}$ aggregation (25 μM) by tested inhibitors at 25 μM.

[c] Inhibition of Cu^{2+}-induced A$\beta_{1\text{-}42}$ aggregation. The concentration of tested compounds and Cu^{2+} were 25 μM.

[d] Percentages are the percent inhibition of MAO by tested compounds at 10 μM.

[e] SI = IC_{50} (MAO-A) / IC_{50} (MAO-B)

[f] The data are expressed as μM of Trolox equiv/μM of tested compound.

[g] The mean ± SD of the three independent experiments.

2.2.2. Recombinant human MAO-A and –B inhibition studies

Subsequently, we evaluated these compounds for their potential MAO-A and -B inhibitory properties. Recombinant human MAO-A and -B were employed as enzyme sources, with clorgyline, rasagiline and iproniazid as reference compounds. Kynuramine, the common substrate for MAO-A and -B, was used for the enzyme activity measurement of both isozymes. Kynuramine is oxidized by the isozymes to yield 4-hydroxyquinoline which fluoresces in the alkaline medium used to terminate the enzymatic reactions.[39-41] The concentrations of 4-hydroxyquinoline in the reactions were measured using fluorescence spectrophotometry without interference from kynuramine or test compounds. We first tested our derivatives at the concentration of 10 μM for preliminary screening. The samples with the inhibition ratios greater than 50% would be retested for the IC_{50} values at various concentrations. All determinations were carried out in triplicate. The results were summarized in **Table 1**. As it shown, most of the aurone derivatives were effective in inhibiting MAO in submicromolar range. Compound **14b** was the most potent MAO-A inhibitor with an IC_{50} of 0.0279 ± 0.004 μM. And the most potent MAO-B inhibitor was **15b** (IC_{50} = 0.226 ± 0.017 μM).

From the results of **14a-g**, we could find that cyclic amine substituted aurones exhibited MAO-B selective inhibitory activities, while the non-cyclic amine substituted aurones preferred MAO-A. Different from the conclusion of A$\beta_{1\text{-}42}$ aggregation assays, the comparison between the potencies of **14a** and **14h** derived that the substituted sites were of great importance and the 4'-substituted aurones were more effective. Interestingly, when the hydroxyl group at the 6-position of aurone (**14a**, **14e** and **14f**) was replaced by a methoxy group (**15a-c**), the inhibitory activity to MAO-A decreased dramatically. On the contrary, the MAO-B inhibitory potencies increased or showed no significant change. As a result, the selectivity to MAO-B was remarkably elevated. It indicated that the hydroxyl group at 6-position of aurone was critical to the MAO-A inhibitory activity, while 6-methoxy group was beneficial to the MAO-B selectively inhibition. The low potency of **17** suggested that only hydroxyl or methoxy group at 6-position was profitable. From the results of **16a** and **16b**, we concluded that the α,β-unsaturated ketone skeleton of aurone was indispensable, consistent with the above conclusion of A$\beta_{1\text{-}42}$ aggregation assays.

2.2.3. Molecular modeling study

In order to explore the hypothetical binding modes of the aurone derivatives with respect to both isoforms of human MAO, docking simulations were carried out using the docking program, AutoDock 4.2 package with Discovery Studio 2.5 based on the X-ray crystal structures of human MAO-A (PDB code: 2Z5X) and MAO-B (PDB code: 2V60). Taking into account the experimental hMAO inhibition data and the resulting structure-activity relationship, compounds **14e** and **15b** were chosen for our molecular modeling investigation. And the most stable binding modes of both compounds in the hMAO-A and -B active sites were graphically inspected (**Figure 3** and **4**). As shown in **Figure 3**, the benzofuran-3(2*H*)-one moieties of **14e** and **15b** were close to the FAD cofactor, adopting parallel π-π interactions with Tyr407. And the B-rings of both **14e** and **15b** adopted parallel π-π interactions with Phe208. In **Figure 3A**, the 6-OH of **14e** was involved in two hydrogen bonds between Asn181 and Tyr444 (Asn181=O • • • HO-**14e**; Tyr444-OH • • • O-**14e**). While in **Figure 3B**, one hydrogen bond was generated between the 6-OCH_3 of **15b** and Tyr444 (Tyr444-OH • • • O-**15b**). This could explain the critical function of hydroxyl group at the 6-position and the significant difference between the MAO-A inhibitory activities of **14e** and **15b**. Meanwhile, both **14e** and **15b** interacted with many other amino acids, such as Tyr69, Leu97, Ala111, Ile180, Val210, Gln215, Cys323, Ile325, Ile335, Leu337, Phe352 and so on.

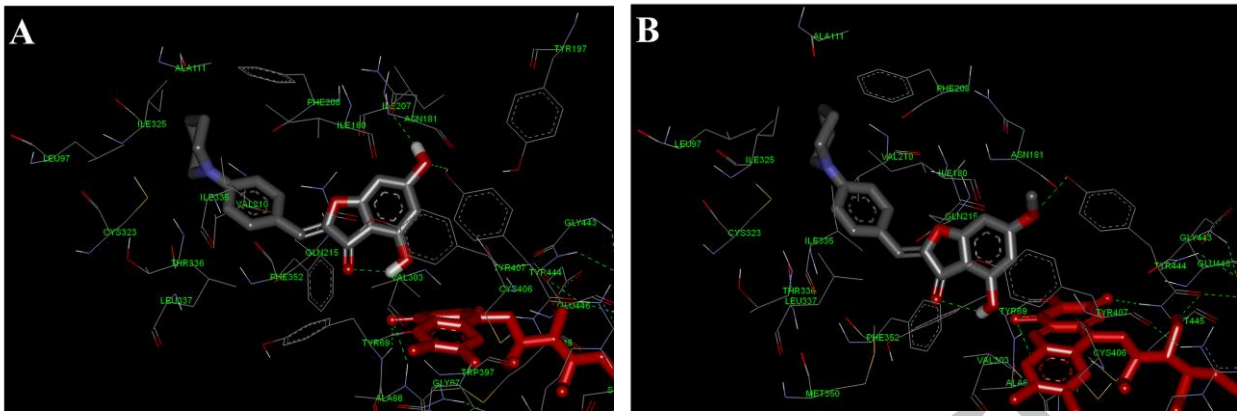

Figure 3. Representation of compound **14e** (**A**) and **15b** (**B**) docked into the binding site of hMAO-A, highlighting the protein residues that participate in the main interactions with the inhibitor. Hydrogen-bonds are shown with the green dotted lines. Pictures were generated with Discovery Studio 2.5. (For interpretation of the references to colour in this figure legend, the reader is referred to the web version of this article.)

In both **14e**- and **15b**-hMAO-B complexes, the interaction pattern was similar (**Figure 4**). From **Figure 4A**, it could be found that four hydrogen bonds were generated between the ligand **14e** and the active site of hMAO-B: two between the hydroxyl group at 4-position and Tyr435-OH (Tyr435-OH • • • O-**14e**; Tyr435-O • • • HO-**14e**), one between the carbonyl group at 3-position and Tyr435-OH (Tyr435-OH • • • O=**14e**) and one between the hydroxyl group at 6-position and the FAD N5 atom (FAD-N5 • • • OH-**14e**). Similarly in **15b**-hMAO-B complex (**Figure 4B**), the hydroxyl group at 4-position and carbonyl group at 3-position interacted with Cys172 and Tyr435 via four hydrogen bonds in total (Cys172=O • • • HO-**15b**; Cys172-SH • • • O=**15b**; Tyr435-OH • • • O=**15b**; Tyr435-O • • • HO-**15b**). Moreover, in both **14e**- and **15b**-hMAO-B complexes, the benzofuran-3(2*H*)-one moieties and B-rings interacted with Tyr398 and Tyr326 via parallel π-π interactions, respectively. Other interactions could be observed between the ligands (**14e** and **15b**) and Pro102, Pro104, Phe168, Leu171, Ile198, Ile199, Gln206, Ile316, Phe343 and so on. The docking studies, consistent with the conclusion resulting from the hMAO inhibition assay, explained the high MAO inhibitory activity and the MAO-B selectivity of these aurone derivatives.

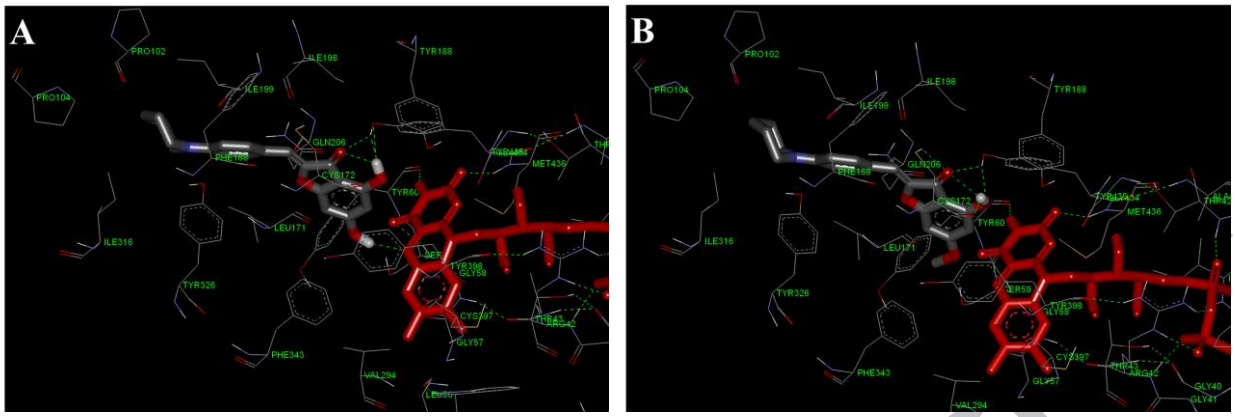

Figure 4. Representation of compound **14e** (**A**) and **15b** (**B**) docked into the binding site of hMAO-B, highlighting the protein residues that participate in the main interactions with the inhibitor. Hydrogen-bonds are shown with the green dotted lines. Pictures were generated with Discovery Studio 2.5. (For interpretation of the references to colour in this figure legend, the reader is referred to the web version of this article.)

2.2.4. Antioxidant activity assay

The antioxidant activities of aurone derivatives were evaluated by the well-established ORAC-FL method (oxygen radical absorbance capacity by fluorescein)[42] with the results shown in **Table 1**. Trolox, a water-soluble vitamin E analog, was used as the standard. And the activities of tested compounds to scavenge radicals were expressed as Trolox equivalent. Their relative activities at concentration of 5 μM were compared with the highly potent compound Trolox. All the tested derivatives exhibited high peroxyl radical absorbance capacities, ranging from 1.00 to 3.56-fold of Trolox. Upon the comparison of the results of **14a-h** with that of **15a-c**, it was apparent that the dihydroxy aurone derivatives (except for **14d**) possessed higher antioxidant potencies than the monohydroxy aurones. It could be found that the reduction products **16a** and **16b** displayed excellent antioxidant activities, higher than other derivatives. The results of **14a**, **15a** and **17** (ORAC-FL values of 2.90 ± 0.03, 1.62 ± 0.08 and 2.43 ± 0.12 equiv, respectively) demonstrated that the introduction of dimethylamino group at 6-position was important to the improvement of antioxidant activity, although the potency of **17** was slightly inferior to that of **14a**. Among the tested compounds, **16b** showed the most potent antioxidant activity with ORAC-FL values of 3.56 ± 0.14 Trolox equivalents.

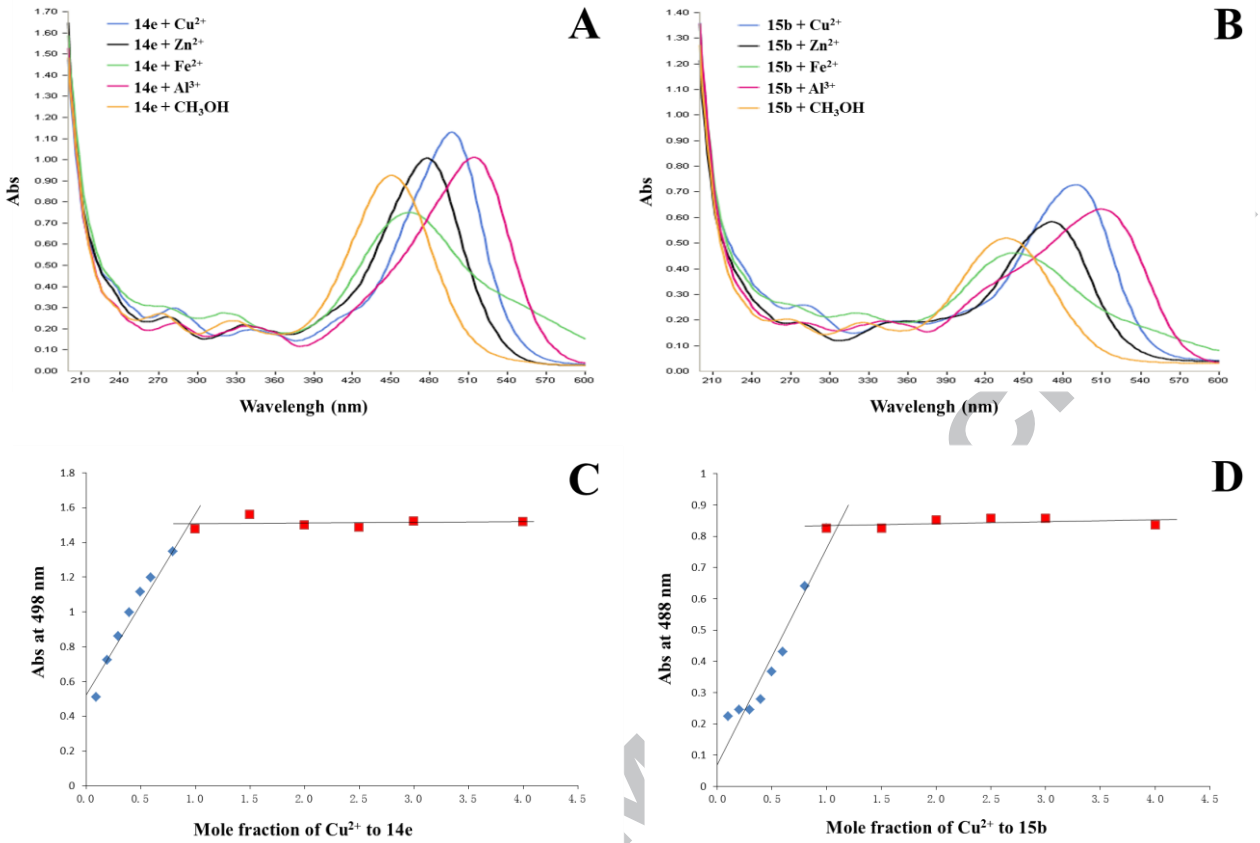

Figure 5. UV spectra of compound **14e** (**A**) and **15b** (**B**) (37.5 μM in methanol) alone or in the presence of $CuCl_2$, $ZnCl_2$, $FeSO_4$ or $AlCl_3$ (37.5 μM, in methanol). Determination of the stoichiometry of complex-Cu^{2+} by using the molar ratio method of titrating the methanol solution of compound **14e** (**C**) and **15b** (**D**) with ascending amounts of $CuCl_2$. The final concentration of tested compound was 37.5 μM, and the final concentration of Cu^{2+} ranged from 3.75 to 150 μM.

2.2.5. Metal-chelating studies

In addition, **14e** and **15b** were chosen as representatives to evaluate the metal chelating abilities toward biometals such as Cu^{2+}, Zn^{2+}, Fe^{2+} and Al^{3+} using UV-visual spectrometry. The results were shown in **Figure 5**. It could be seen that, the spectrum of **14e** was significantly altered upon the addition of $CuCl_2$, $ZnCl_2$ and $AlCl_3$ (**Figure 5A**). When $CuCl_2$ was added, a red shift in the maximum absorption from 450 nm to 498 nm occurred, indicating the formation of a **14e**-Cu^{2+} complex. The similar red shifts were also observed when $ZnCl_2$ and $AlCl_3$ were added. However, no significant shift occurred with the addition of $FeSO_4$. The chelating effect could be reasonably attributed to the 3-carbonyl and 4-hydroxyl groups in aurone. Similar results were observed for **15b** (**Figure 5B**). The molar ratio method was performed to determine the stoichiometry of **14e**-Cu^{2+} and **15b**-Cu^{2+} complexes, by preparing the methanol solutions of **14e** and **15b** with ascending amounts of $CuCl_2$.

The UV spectra were used to obtain the absorbance of the **14e** and **15b** complexes and different concentrations of $CuCl_2$ at 498 nm and 488 nm respectively. The results showed that absorbance linearly increased initially and then plateaued (**Figure 5C** and **5D**). The points for the straight lines to intersect were determined to be at a mole proportion of 0.95 and 1.11 respectively, revealing a 1:1 stoichiometry for **14e**-Cu^{2+} and **15b**-Cu^{2+} complexes.

2.2.6. In vitro blood-brain barrier permeation assay

An important prerequisite of any compound to act on neurodegenerative processes is to cross the blood-brain barrier (BBB) and penetrate into the brain. To predict the possible *in vivo* BBB permeability of the aurone derivatives, the parallel artificial membrane permeation assay of the blood-brain barrier (PAMPA-BBB) was performed[43,44] and **14e** and **15b** were still chosen as representatives. Assay validation was made by comparing experimental permeabilities of 11 commercial drugs with reported values (**Table 2**). A plot of experimental data versus bibliographic values gave a good linear correlation, P_e (exp.) = 0.9163 × P_e (bibl.) − 0.2247 (R^2 = 0.9558) (**Figure 6**). From this equation and taking into account the limit established by Di et al.[43] for BBB permeation, we determined that compounds with P_e values above 3.44 × 10^{-6} cm/s could cross the BBB (**Table 3**). The result in **Table 4** indicated that **14e** and **15b** would be able to penetrate the BBB and reach the therapeutic targets in central nervous system (CNS).

Table 2. Permeability P_e (× 10^{-6} cm/s) in the PAMPA-BBB assay for 11 commercial drugs used in the experiment validation.

Commercial drugs	Bibl[a]	PBS/EtOH (70:30)[b]
Verapamil	16	16.90 ± 0.36
Oxazepam	10	9.60 ± 0.21
Diazepam	16	11.86 ± 0.23
Clonidine	5.3	5.10 ± 0.16
Imipramine	13	10.10 ± 0.22
Testosterone	17	16.30 ± 0.25
Caffeine	1.3	1.28 ± 0.05
Enoxacine	0.9	0.47 ± 0.01
Piroxicam	2.5	0.72 ± 0.02
Norfloxacin	0.1	0.42 ± 0.01
Theophylline	0.12	0.10 ± 0.003

[a] Taken from Ref.[43]

[b] Data are the mean ± SD of three independent experiments.

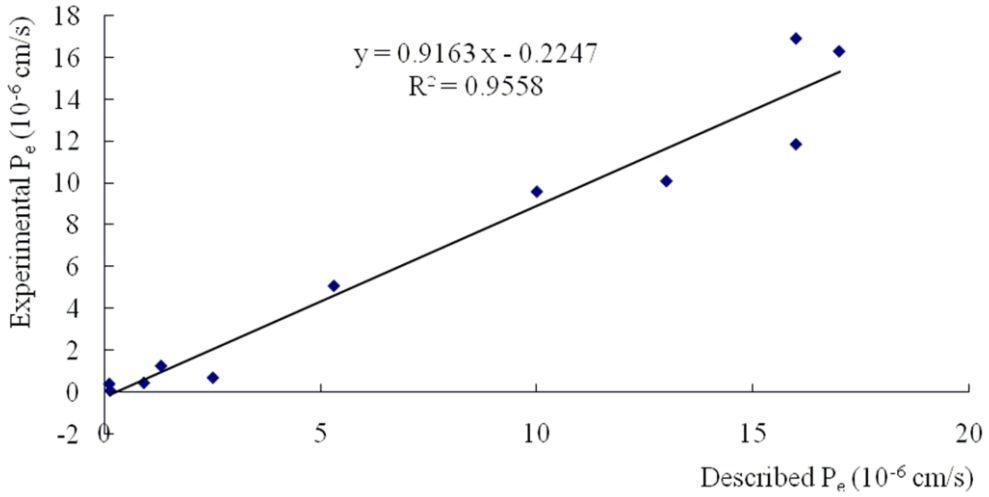

Figure 6. Lineal correlation between experimental and reported permeability of commercial drugs using the PAMPA-BBB assay. P_e (exp) = 0.9163 × P_e (bibl.) − 0.2247 (R^2 = 0.9558).

Table 3. Ranges of permeability of PAMPA-BBB assays (P_e × 10^{-6} cm/s).

High BBB permeation predicted (CNS +)	$P_e > 3.44$
Uncertain BBB permeation (CNS +/-)	$3.44 > P_e > 1.61$
Low BBB permeation predicted (CNS -)	$P_e < 1.61$

Table 4. Permeability results P_e (× 10^{-6} cm/s) from the PAMPA-BBB assay for selected aurone derivatives with their predicted penetration into the CNS.

Compd.[a]	P_e (× 10^{-6} cm/s)[b]	Prediction
14e	6.68 ± 0.29	CNS +
15b	7.24 ± 0.22	CNS +

[a] Compound **14e** and **15b** were dissolved in DMSO at 5 mg/mL and diluted with PBS/EtOH (70:30). The final concentration of each compound was 100 μg/mL.

[b] Data are the mean ± SD of three independent experiments.

3. Conclusion

In conclusion, a series of aurone derivatives were designed, synthesized and evaluated as multifunctional agents for the treatment of AD. We observed that all the compounds exhibited moderate to good inhibitory activities of self- and Cu^{2+}-induced Aβ_{1-42} aggregation. And most of them were effective in inhibiting MAO in submicromolar range. Furthermore, **15a-c** exhibited high selectivity to MAO-B over MAO-A, which may serve as potential MAO-B selective inhibitors. All

of the tested derivatives showed high antioxidant activities, ranging from 1.00 to 3.56-fold of Trolox, revealing their potential abilities to decrease the oxidative damage. Moreover, the representative compounds **14e** and **15b** showed good metal-chelating properties and BBB permeabilities. These properties indicate that the aurone derivatives may provide a good template for the development of new multifunctional anti-AD agents.

4. Experimental section

4.1. Chemistry

Unless otherwise noted, all materials were obtained from commercial suppliers and used without further purification. The ^{1}H NMR and ^{13}C NMR spectra were recorded using TMS as the internal standard in DMSO-d_6 on a Varian INOVA spectrometer at 25 °C. Coupling constants are given in Hz. MS spectra data were obtained on an Agilent-6210 TOF LC-MS spectrometer. Melting points (uncorrected) were measured on YRT-3 melting-point apparatus (China). Reaction progress was monitored by thin-layer chromatography (TLC) using silica gel GF_{254} plates from Qingdao Haiyang Chemical Co. Ltd. (China) and the spots were detected under UV light (254 nm). Column chromatography was performed with silica gel (230–400 mesh) purchased from Qingdao Haiyang Chemical Co. Ltd. (China).

4.1.1. Synthesis of 2-chloro-1-(2,4,6-trihydroxyphenyl)ethanone (4)

Anhydrous phloroglucinol (**3**, 5.02 g, 39.8 mmol) was dissolved in EtOAc (75 mL). $AlCl_3$ (21.1 g, 158 mmol) was added at room temperature to give a pale brown suspension. The reaction mixture was stirred at room temperature for 30 min. Chloroacetyl chloride (3.28 mL, 43.6 mmol) was added, and the reaction mixture was stirred at room temperature overnight and then heated at 50 °C for 6 h. The reaction mixture was quenched by pouring into ice-water and the product was extracted with EtOAc (6 × 60 mL), then washed with brine, dried over Na_2SO_4, filtered and concentrated under reduced pressure to give compound **4** (6.25 g) as a pale yellow solid, which was used without further purification.

4.1.2. Synthesis of 4,6-dihydroxybenzofuran-3(2*H*)-one (5)

Compound **4** (6.25 g) was dissolved in methanol (94 mL) and anhydrous NaOAc (5.34 g, 65.1 mmol) was added. The reaction mixture was then refluxed under argon atmosphere for 4 h. The methanol was evaporated and the residue was recrystallized from water to give compound **5** (4.54 g,

88.2%) as a pale yellow solid. ^{1}H NMR (400 MHz, DMSO-d_6) δ 10.62 (brs, 2H), 5.91 (s, 2H), 4.54 (s, 2H). (Data are in agreement with references[28].)

4.1.3. Synthesis of 4-hydroxy-6-methoxybenzofuran-3(2*H*)-one (7)

Compound **7** was obtained by the dimethylation of **5** and subsequent selective deprotection using the method reported previously.[33] mp 139-141 °C (lit.[33] 140-142 °C).

4.1.4. General procedure for the synthesis of 8a-h

Compounds **8b-h** were prepared as previously described.[32] Compound **8a** was obtained from commercial supplier.

4.1.5. General procedure for the synthesis of 14a-h and 15a-c

To a solution of **5** or **7** in ethanol (3 mL/mmol) were added an aqueous solution of potassium hydroxide (50%, 5 mL/mmol) and a benzaldehyde derivative (**8a-h**, 1.5 equiv.) The solution was stirred overnight until TLC showed complete disappearance of the starting material. Ethanol was removed under reduced pressure. The residue was diluted into distilled water and acidified with an aqueous solution of hydrochloric acid (10%), then the mixture was basified with saturated $NaHCO_3$ solution to adjust the pH to 7-8. The precipitate was filtered, washed with water and dried at room temperature to afford the corresponding crude aurone derivative as orange to dark red solid.

4.1.5.1. (*Z*)-2-(4-(dimethylamino)benzylidene)-4,6-dihydroxybenzofuran-3(2*H*)-one (14a)

Compound **14a** was synthesized from 4,6-dihydroxybenzofuran-3(2*H*)-one (**5**) and benzaldehyde derivative **8a** according to the general procedure. After purification by chromatagraphy on silica gel using petroleum ether/acetone (2:1) as eluent, the pure product **14a** was obtained as a red solid, yield 60.7%. ^{1}H NMR (600 MHz, DMSO-d_6) δ 10.77 (s, 1H), 10.75 (s, 1H), 7.74 (d, J = 7.8 Hz, 2H), 6.79 (d, J = 7.8 Hz, 2H), 6.54 (s, 1H), 6.20 (s, 1H), 6.07 (s, 1H), 3.00 (s, 6H). (Data are in agreement with references[2].) HR-ESI-MS: Calcd. for $C_{17}H_{16}NO_4$ $[M + H]^+$: 298.1079, found : 298.1078.

4.1.5.2. (*Z*)-2-(4-(ethyl(methyl)amino)benzylidene)-4,6-dihydroxybenzofuran-3(2*H*)-one (14b)

Compound **14b** was synthesized from 4,6-dihydroxybenzofuran-3(2*H*)-one (**5**) and benzaldehyde derivative **8b** according to the general procedure. After purification by chromatagraphy on silica gel using petroleum ether/acetone (2:1) as eluent, the pure product **14b** was obtained as a dark red solid, yield 38.1%. ^{1}H NMR (600 MHz, DMSO-d_6) δ 10.82 (brs, 2H), 7.72 (d,

J = 7.8 Hz, 2H), 6.77 (d, *J* = 7.8 Hz, 2H), 6.52 (s, 1H), 6.17 (s, 1H), 6.06 (s, 1H), 3.46 (s, 2H), 2.95 (s, 3H), 1.07 (s, 3H). HR-ESI-MS: Calcd. for $C_{18}H_{18}NO_4$ $[M + H]^+$: 312.1236, found : 312.1238.

4.1.5.3. (*Z*)-2-(4-(diethylamino)benzylidene)-4,6-dihydroxybenzofuran-3(2*H*)-one (14c)

Compound **14c** was synthesized from 4,6-dihydroxybenzofuran-3(2*H*)-one (**5**) and benzaldehyde derivative **8c** according to the general procedure. After purification by chromatagraphy on silica gel using dichloromethane/methanol (10:1) as eluent, the pure product **14c** was obtained as a dark red solid, yield 50.0%. ^{1}H NMR (400 MHz, DMSO-d_6) δ 10.75 (brs, 2H), 7.71 (d, *J* = 8.8 Hz, 2H), 6.73 (d, *J* = 8.8 Hz, 2H), 6.51 (s, 1H), 6.18 (s, 1H), 6.06 (s, 1H), 3.41-3.36 (m, 4H), 1.12 (t, *J* = 7.2 Hz, 6H). HR-ESI-MS: Calcd. for $C_{19}H_{20}NO_4$ $[M + H]^+$: 326.1392, found : 326.1399.

4.1.5.4. (*Z*)-4,6-dihydroxy-2-(4-(pyrrolidin-1-yl)benzylidene)benzofuran-3(2*H*)-one (14d)

Compound **14d** was synthesized from 4,6-dihydroxybenzofuran-3(2*H*)-one (**5**) and benzaldehyde derivative **8d** according to the general procedure. After purification by chromatagraphy on silica gel using petroleum ether/acetone (2:1) as eluent, the pure product **14d** was obtained as a dark red solid, yield 36.3%. ^{1}H NMR (400 MHz, DMSO-d_6) δ 10.90 (brs, 2H), 7.72 (brs, 2H), 6.61 (brs, 2H), 6.51 (s, 1H), 6.15 (s, 1H), 6.02 (s, 1H), 3.36 (brs, 4H), 1.96 (brs, 4H). HR-ESI-MS: Calcd. for $C_{19}H_{18}NO_4$ $[M + H]^+$: 324.1236, found : 324.1234.

4.1.5.5. (*Z*)-4,6-dihydroxy-2-(4-(piperidin-1-yl)benzylidene)benzofuran-3(2*H*)-one (14e)

Compound **14e** was synthesized from 4,6-dihydroxybenzofuran-3(2*H*)-one (**5**) and benzaldehyde derivative **8e** according to the general procedure. After purification by chromatagraphy on silica gel using dichloromethane/methanol (15:1) as eluent, the pure product **14e** was obtained as a dark red solid, yield 47.1%. ^{1}H NMR (400 MHz, DMSO-d_6) δ 10.78 (brs, 2H), 7.73 (d, *J* = 8.8 Hz, 2H), 6.98 (d, *J* = 8.8 Hz, 2H), 6.52 (s, 1H), 6.19 (s, 1H), 6.06 (s, 1H), 3.34 (s, 4H), 1.59 (s, 6H). (Data are in agreement with references[28].) HR-ESI-MS: Calcd. for $C_{20}H_{20}NO_4$ $[M + H]^+$: 338.1392, found : 338.1398.

4.1.5.6. (*Z*)-4,6-dihydroxy-2-(4-morpholinobenzylidene)benzofuran-3(2*H*)-one (14f)

Compound **14f** was synthesized from 4,6-dihydroxybenzofuran-3(2*H*)-one (**5**) and benzaldehyde derivative **8f** according to the general procedure. After purification by chromatagraphy on silica gel using dichloromethane/methanol (15:1) as eluent, the pure product **14f** was obtained as an orange red solid, yield 19.6%. ^{1}H NMR (600 MHz, DMSO-d_6) δ 10.86 (brs, 2H), 7.77 (d, *J* = 8.4 Hz, 2H), 7.02 (d, *J* = 8.4 Hz, 2H), 6.55 (s, 1H), 6.21 (s, 1H), 6.08 (s, 1H), 3.75 (t, *J* = 4.8 Hz, 4H),

3.24 (t, *J* = 4.8 Hz, 4H). (Data are in agreement with references[30].) HR-ESI-MS: Calcd. for $C_{19}H_{18}NO_5$ $[M + H]^+$: 340.1185, found : 340.1192.

4.1.5.7. (*Z*)-4,6-dihydroxy-2-(4-(4-methylpiperazin-1-yl)benzylidene)benzofuran-3(2*H*)-one (14g)

Compound **14g** was synthesized from 4,6-dihydroxybenzofuran-3(2*H*)-one (**5**) and benzaldehyde derivative **8g** according to the general procedure. After purification by chromatagraphy on silica gel using dichloromethane/methanol (8:1) as eluent, the pure product **14g** was obtained as an orange red solid, yield 10.1%. ^{1}H NMR (400 MHz, DMSO-d_6) δ 10.80 (brs, 2H), 7.75 (d, *J* = 8.8 Hz, 2H), 7.02 (d, *J* = 8.8 Hz, 2H), 6.52 (s, 1H), 6.21 (s, 1H), 6.10 (s, 1H), 3.51 (brs, 4H), 2.51 (brs, 4H), 2.27 (s, 3H). HR-ESI-MS: Calcd. for $C_{20}H_{21}N_2O_4$ $[M + H]^+$: 353.1501, found : 353.1512.

4.1.5.8. (*Z*)-2-(2-(dimethylamino)benzylidene)-4,6-dihydroxybenzofuran-3(2*H*)-one (14h)

Compound **14h** was synthesized from 4,6-dihydroxybenzofuran-3(2*H*)-one (**5**) and benzaldehyde derivative **8h** according to the general procedure. After purification by chromatagraphy on silica gel using dichloromethane/methanol (10:1) as eluent, the pure product **14h** was obtained as an orange red solid, yield 64.8%. ^{1}H NMR (400 MHz, DMSO-d_6) δ 10.94 (brs, 2H), 8.03 (d, *J* = 7.2 Hz, 1H), 7.35 (t, *J* = 7.2 Hz, 1H), 7.17-7.11 (m, 2H), 6.86 (s, 1H), 6.20 (s, 1H), 6.08 (s, 1H).2.71 (s, 6H). ^{13}C NMR (150 MHz, DMSO-d_6) δ 179.5, 168.0, 167.6, 158.7, 154.1, 147.7, 131.1, 130.2, 125.6, 122.7, 119.0, 105.1, 103.0, 97.9, 90.7, 45.1 (2C). HR-ESI-MS: Calcd. for $C_{17}H_{16}NO_4$ $[M + H]^+$: 298.1079, found : 298.1078.

4.1.5.9. (*Z*)-2-(4-(dimethylamino)benzylidene)-4-hydroxy-6-methoxybenzofuran-3(2*H*)-one (15a)

Compound **15a** was synthesized from 4-hydroxy-6-methoxybenzofuran-3(2*H*)-one (**7**) and benzaldehyde derivative **8a** according to the general procedure. After purification by chromatagraphy on silica gel using dichloromethane/methanol (20:1) as eluent, the pure product **15a** was obtained as an orange red solid, yield 15.6%. ^{1}H NMR (400 MHz, DMSO-d_6) δ 10.96 (brs, 1H), 7.76 (d, *J* = 8.4 Hz, 2H), 6.77 (d, *J* = 8.4 Hz, 2H), 6.59 (s, 1H), 6.48 (s, 1H), 6.12 (s, 1H), 3.83 (s, 3H), 2.99 (s, 6H). HR-ESI-MS: Calcd. for $C_{18}H_{18}NO_4$ $[M + H]^+$: 312.1236, found : 312.1241.

4.1.5.10. (*Z*)-4-hydroxy-6-methoxy-2-(4-(piperidin-1-yl)benzylidene)benzofuran-3(2*H*)-one (15b)

Compound **15b** was synthesized from 4-hydroxy-6-methoxybenzofuran-3(2*H*)-one (**7**) and benzaldehyde derivative **8e** according to the general procedure. After purification by chromatagraphy on silica gel using dichloromethane/methanol (20:1) as eluent, the pure product **15b** was obtained as an orange red solid, yield 53.3%, mp 200-201 °C. ^{1}H NMR (400 MHz, DMSO-d_6) δ 11.00 (brs, 1H), 7.75 (d, J = 8.0 Hz, 2H), 6.99 (d, J = 8.0 Hz, 2H), 6.58 (s, 1H), 6.48 (s, 1H), 6.11 (s, 1H), 3.83 (s, 3H), 3.32 (s, 4H), 1.59 (s, 6H). ^{13}C NMR (150 MHz, DMSO-d_6) δ 179.4, 168.0, 167.5, 158.2, 151.7, 145.8, 132.7 (2C), 121.2, 114.7 (2C), 110.4, 104.5, 97.0, 88.8, 56.2, 48.3 (2C), 25.2 (2C), 24.2. HR-ESI-MS: Calcd. for $C_{21}H_{22}NO_4$ $[M + H]^+$: 352.1549, found : 352.1553.

4.1.5.11. (*Z*)-4-hydroxy-6-methoxy-2-(4-morpholinobenzylidene)benzofuran-3(2*H*)-one (15c)

Compound **15c** was synthesized from 4-hydroxy-6-methoxybenzofuran-3(2*H*)-one (**7**) and benzaldehyde derivative **8f** according to the general procedure. After purification by chromatagraphy on silica gel using dichloromethane/methanol (20:1) as eluent, the pure product **15c** was obtained as an orange red solid, yield 61.6%, mp 228 °C (decomposed). ^{1}H NMR (400 MHz, DMSO-d_6) δ 11.10 (brs, 1H), 7.80 (d, J = 8.0 Hz, 2H), 7.02 (d, J = 8.0 Hz, 2H), 6.60 (s, 1H), 6.48 (s, 1H), 6.10 (s, 1H), 3.83 (s, 3H), 3.75 (s, 4H), 3.25 (s, 4H). ^{13}C NMR (150 MHz, DMSO-d_6) δ 179.4, 168.1, 167.6, 158.3, 151.6, 146.0, 132.5 (2C), 122.4, 114.5 (2C), 110.1, 104.3, 97.0, 89.0, 66.1 (2C), 56.3, 47.4 (2C). HR-ESI-MS: Calcd. for $C_{20}H_{20}NO_5$ $[M + H]^+$: 354.1341, found : 354.1346.

4.1.6. General procedure for the synthesis of 16a and 16b

A mixture of compound **14a** or **14f** (100 mg) in THF (2 mL) and 10% palladium on carbon (10 mg) was stirred under hydrogen (balloon) overnight. The mixture was then filtered and the filtrate was concentrated to give crude product **16a** or **16b** as brown oil. Purification by chromatagraphy on silica gel using dichloromethane/methanol as eluent afforded the pure product **16a** or **16b**.

4.1.6.1. 2-(4-(dimethylamino)benzyl)-4,6-dihydroxybenzofuran-3(2*H*)-one (16a)

Compound **16a** was synthesized from Compound **14a** according to the general procedure. After purification by chromatagraphy on silica gel using dichloromethane/methanol (15:1) as eluent, the pure product **16a** was obtained as an almost white solid, yield 52.5%, mp 193-195 °C. ^{1}H NMR (400 MHz, DMSO-d_6) δ 10.57 (brs, 2H), 7.05 (d, J = 8.4 Hz, 2H), 6.62 (d, J = 8.4 Hz, 2H), 5.86 (s, 1H), 5.85 (s, 1H), 4.73 (dd, J_1 = 7.6 Hz, J_2 = 3.6 Hz, 1H), 3.04 (dd, J_1 = 14.8 Hz, J_2 = 3.6 Hz, 1H), 2.83 (s, 6H), 2.73 (dd, J_1 = 14.8 Hz, J_2 = 7.6 Hz, 1H). ^{13}C NMR (100 MHz, DMSO-d_6) δ 195.0, 174.4, 168.0,

157.9, 149.4, 130.1 (2C), 124.1, 112.5 (2C), 102.7, 96.3, 90.1, 86.0, 40.4 (2C), 36.1. HR-ESI-MS: Calcd. for $C_{17}H_{18}NO_4$ $[M + H]^+$: 300.1236, found : 300.1240.

4.1.6.2. 4,6-dihydroxy-2-(4-morpholinobenzyl)benzofuran-3(2*H*)-one (16b)

Compound **16b** was synthesized from Compound **14f** according to the general procedure. After purification by chromatagraphy on silica gel using dichloromethane/methanol (20:1) as eluent, the pure product **16b** was obtained as a pale yellow solid, yield 20.5%, mp 197-199 °C. ^{1}H NMR (400 MHz, DMSO-d_6) δ 10.59 (brs, 2H), 7.10 (d, J = 8.4 Hz, 2H), 6.83 (d, J = 8.4 Hz, 2H), 5.87 (s, 1H), 5.85 (s, 1H), 4.76 (dd, J_1 = 8.4 Hz, J_2 = 3.6 Hz, 1H), 3.71 (s, 4H), 3.09-3.04 (m, 5H), 2.75 (dd, J_1 = 14.8 Hz, J_2 = 8.4 Hz, 1H). ^{13}C NMR (150 MHz, DMSO-d_6) δ 194.9, 174.4, 168.0, 157.9, 149.9, 130.1 (2C), 127.2, 115.1 (2C), 102.7, 96.3, 90.1, 85.8, 71.5 (2C), 48.7 (2C), 36.1. HR-ESI-MS: Calcd. for $C_{19}H_{20}NO_5$ $[M + H]^+$: 342.1341, found : 342.1345.

4.1.7.(*E*)-1-(4-(dimethylamino)-2-hydroxy-6-methoxyphenyl)-3-(4-(dimethylamino)phenyl)prop-2-en-1-one (12)

The synthesis of **11** starting from anhydrous phloroglucinol (**4**) was reported by our group previously.[6] Compound **12** was synthesized from compound **11** and *p*-dimethylaminobenzaldehyde (**8a**) in the same manner to **14a-h** and **15a-c** as a brown oil, and the crude product was used without further purification.

4.1.8.(*Z*)-6-(dimethylamino)-2-(4-(dimethylamino)benzylidene)-4-methoxybenzofuran-3(2H)-one (13)

To a solution of chalcone **12** (204 mg) in pyridine (6 mL) was added $Hg(OAc)_2$ (191 mg, 0.600 mmol) at room temperature, and the mixture was refluxed for 15 h. The cooled reaction mixture was poured into ice-cold water (20 mL) and extracted with EtOAc (5 × 20 mL), then washed with brine, dried over Na_2SO_4, filtered and concentrated under reduced pressure to give crude compound **13** (249 mg) as a dark red solid, which was used without further purification.

4.1.9.(*Z*)-6-(dimethylamino)-2-(4-(dimethylamino)benzylidene)-4-hydroxybenzofuran-3(2H)-one (17)

Compound **13** (100 mg) was dissolved in an aqueous solution of hydrobromic acid (40%, 2 mL) and the solution was heated at 100 °C for 2 h. The cooled mixture was basified with saturated $NaHCO_3$ solution to adjust the pH to 7 and extracted with CH_2Cl_2 (5 × 10 mL), then washed with brine, dried over Na_2SO_4, filtered and concentrated under reduced pressure to give the crude product

as a brown solid. After purification by chromatagraphy on silica gel using dichloromethane/methanol (30:1) as eluent, the pure product **17** (15 mg) was obtained as a dark red solid. ^{1}H NMR (400 MHz, DMSO-d_6) δ 10.45 (brs, 1H), 77.2 (d, J = 7.6 Hz, 2H), 6.76 (d, J = 7.6 Hz, 2H), 6.42 (s, 1H), 6.12 (s, 1H), 5.83 (s, 1H), 3.03 (s, 6H), 2.98 (s, 6H). ^{13}C NMR (150 MHz, DMSO-d_6) δ 178.0, 167.4, 157.6, 150.6, 146.2, 132.2 (2C), 120.2, 112.2 (2C), 108.6, 100.3, 93.0, 86.0, 40.3 (2C), 39.9 (2C). HR-ESI-MS: Calcd. for $C_{19}H_{21}N_2O_3$ $[M + H]^+$: 325.1552, found : 325.1558.

4.2. Biological activity

4.2.1. Inhibition of self- and Cu^{2+}-induced A$\beta_{1\text{-}42}$ aggregation

A Thioflavin T-based fluorometric assay was performed to investigate the self-induced A$\beta_{1\text{-}42}$ aggregation.[37,45-46] Thioflavin T (Basic Yellow 1, ThT) was purchased from TCI (Shanghai) Development. β-Amyloid$_{1\text{-}42}$ (A$\beta_{1\text{-}42}$), supplied as trifluoroacetate salt, was purchased from ChinaPeptides Co., Ltd. 1,1,1,3,3,3-hexafluoro-2-propanol (HFIP) was purchased from Energy Chemical. Briefly, A$\beta_{1\text{-}42}$ was dissolved in HFIP (1 mg/mL) and after incubation for 24 h at room temperature, the solvent was evaporated. Then the HFIP pretreated A$\beta_{1\text{-}42}$ was dissolved in dry DMSO to a final stock concentration of 200 μM and was kept frozen at –80 °C until use. Solutions of test compounds were prepared in DMSO in 2.5 mM for storage and diluted with phosphate buffer solution (pH 7.4) before use. For the self-induced assay, A$\beta_{1\text{-}42}$ (20 μL, 25 μM, final concentration) was incubated with 20 μL of test compounds (25 μM, final concentration) in 50 mM phosphate buffer solution (pH 7.40) at 37 °C for 24 h. To minimize evaporation effect the wells were sealed by a transparent heat-resistant plastic film. After incubation, 160 μL of 5 μM ThT in 50 mM glycine-NaOH buffer (pH 8.5) was added. Each assay was run in triplicate. Fluorescence was measured on a Varioskan Flash Multimode Reader (Thermo Scientific) with excitation and emission wavelengths at 446 nm and 490 nm, respectively. The fluorescence intensities were calculated after subtraction of the background activity. The background activity was determined from wells containing all components except A$\beta_{1\text{-}42}$, which were replaced by a phosphate buffer solution (pH 7.40). The percent inhibition due to the presence of the inhibitor was calculated by the following expression: $(1\text{-}IF_i/IF_c) \times 100$, in which IF_i and IF_c are the fluorescence intensities obtained for A$\beta_{1\text{-}42}$ in the presence and in the absence of inhibitors after subtracting the background, respectively.

As for the inhibition of Cu^{2+}-induced A$\beta_{1\text{-}42}$ aggregation[4,47], solutions of Cu^{2+} were prepared

from standards to concentration of 75 μM using the HEPES buffer (20 mM, pH 6.60, 150 mM NaCl) and the A$\beta_{1\text{-}42}$ stock solution was diluted in HEPES buffer (20 mM, pH 6.60, 150 mM NaCl). The mixture of the peptide (20 μL, 25 μM, final concentration) and Cu^{2+} (20 μL, 25 μM, final concentration), with or without the tested compound (20 μL, 25 μM, final concentration) was incubated at 37 °C for 24h. After the incubation, 190 μL of 5 μM ThT in 50 mM glycine-NaOH buffer (pH 8.50) was added. Each assay was run in triplicate. The detection method was the same as that of self-induced A$\beta_{1\text{-}42}$ experiment.

4.2.2. Recombinant human MAO-A and –B inhibition studies

Recombinant human MAO-A and –B (5 mg/mL) were purchased from Sigma-Aldrich, pre-aliquoted and stored at -80 °C. Solutions of test compounds were prepared in DMSO in 2.5 mM for storage and diluted with potassium phosphate buffer (100 mM, pH 7.40, containing KCl 20.2 mM) before use. All the enzymatic reactions were conducted in potassium phosphate buffer (100 mM, pH 7.40, containing KCl 20.2 mM) to a final volume of 500 μL containing kynuramine (45 μM for MAO-A and 30 μM for MAO-B) and various concentrations of test compounds (0-100 μM) with the concentration of DMSO lower than 4%. The reactions were initiated by the addition of MAO-A or MAO-B (7.5 μg/mL) and the solutions were incubated at 37 °C for 30 min. The enzymatic reactions were terminated by the addtion of 400 μL NaOH (2N) and then 1000 μL water, centrifuged for 10 min at 16000 g. The concentrations of the MAO generated 4-hydroxyquinoline in the reactions were determined by measuring the fluorescence of the supernatant on a Varioskan Flash Multimode Reader (Thermo Scientific) with excitation and emission wavelengths at 310 nm and 400 nm, respectively.[39,41] A linear calibration curve was constructed by preparing samples containing 4-hydroxyquinoline (0.047–1.56 μM) dissolved in 500 μL potassium phosphate buffer. To each calibration standard, 400 μL NaOH (2N) and 1000 μL water were added. The appropriate control samples were included to confirm that the test compounds do not fluoresce or quench the fluorescence of 4-hydroxyquinoline under the assay conditions. IC_{50} values were calculated from sigmoidal dose-response curves (graphs of the initial rate of kynuramine oxidation versus the logarithm of inhibitor concentration). Each sigmoidal curve was constructed from six different compound concentrations spanning at least three orders of magnitude. Data analyses were carried out with GraphPad Prism 5 employing the one site competition model. IC_{50} values were determined in triplicate and expressed as mean ± SD.

4.2.3. Molecular modeling study

The simulation systems were built based on the X-ray crystal structures of hMAO-A (PDB code: 2Z5X) and hMAO-B (PDB code: 2V60), both from the Protein Data Bank.[48] The original ligands and water molecules were removed and hydrogen atoms were added onto both proteins and cofactors. Docking studies were performed using Autodock 4.2 program and each docked system was performed by 200 runs of the Autodock search by the Lamarckian genetic algorithm (LGA). A cluster analysis was performed on the docking results using a root mean square (RMS) tolerance of 1.0 and the lowest energy conformation of the highest populated cluster was selected for analysis. Graphic manipulations and visualizations were done by Autodock Tools or Discovery Studio 2.5 software.

4.2.4. Antioxidant activity assay

The antioxidant activity was determined by the oxygen radical absorbance capacity-fluorescein (ORAC-FL) assay.[49] 2,2'-Azobis(amidinopropane) dihydrochloride (AAPH) was purchased from Accela ChemBio Co., Ltd. Fluorescein (FL) and 6-hydroxy-2,5,7,8-tetramethylchromane-2-carboxylic acid (Trolox) were purchased from TCI (Shanghai) Development. All the assays were performed with 75 mM phosphate buffer (pH 7.40), and the final reaction mixture was 200 μL. Antioxidant (20 μL) and fluorescein (120 μL, 150 nM final concentration) were added in the wells of a black 96-well plate with Trolox as a standard (1-8 μM, final concentration). The mixture was pre-incubated for 15 min at 37 °C and then placed in a Varioskan Flash Multimode Reader (Thermo Scientific). AAPH solution (60 μL, 12 mM final concentration) was added rapidly using an autosampler and the fluorescence recorded every minute for 90 min with excitation at 485 nm and emission at 535 nm. The plate was automatically shaken prior to each reading. A blank (FL + AAPH) using phosphate buffer instead of antioxidant and Trolox calibration were carried out in each assay. The samples were measured at different concentrations (1-10 μM). All the reaction mixture was prepared in duplicate, and at least three independent assays were performed for each sample. Antioxidant curves (fluorescence versus time) were normalized to the curve of the blank in the same assay, and then the area under the fluorescence decay curve (AUC) was calculated. The net AUC of a sample was obtained by subtracting the AUC of the blank. ORAC-FL values were expressed as Trolox equivalents by using the standard curve calculated for each sample, where the ORAC-FL value of Trolox was taken as 1, indicating the antioxidant potency of the tested compounds.

4.2.5. Metal-chelating studies[4,50]

The chelating studies were performed with a Varioskan Flash Multimode Reader (Thermo Scientific). The UV absorption spectra of compound (**14e** or **15b**) alone or in the presence of $CuCl_2$, $ZnCl_2$, $AlCl_3$, and $FeSO_4$ were recorded with wavelength ranging from 200 to 600 nm after incubating for 30 min at room temperature. The final volume of reaction mixture was 200 μL, and the final concentrations of tested compound and metals were 37.5 μM. Numerical subtraction of the spectra of the metal alone and the compound alone from the spectra of the mixture gave the difference UV-vis spectra due to complex formation.

The stoichiometry of the compound-Cu^{2+} complex was determined by titrating the methanol solution of tested compound with ascending of $CuCl_2$. The final concentration of tested compound was 37.5 μM, and the final concentration of Cu^{2+} ranged from 3.75 to 150 μM. The UV spectra were recorded and treated by numerical subtraction of $CuCl_2$ and tested compound at corresponding concentrations, plotted versus the mole fraction of tested compound.

4.2.6. In vitro blood-brain barrier permeation assay

The blood-brain barrier penetration of compounds was evaluated using the parallel artificial membrane permeation assay of the blood-brain barrier (PAMPA-BBB) described by Di et al.[43] Commercial drugs were purchased from Sigma and Alfa Aesar. And porcine brain lipid (PBL) was purchased from Avanti Polar Lipids. The donor plate (MATRNPS50) and the acceptor plate (PVDF membrane, pore size 0.45 μm, MAIPN4550) were purchased from Millipore. Filter PDVF membrane units (diameter 25 mm, pore size 0.45 μm) from Pall Corporation were used to filter the samples. Test compounds were dissolved in DMSO at 5 mg/mL and diluted 50-fold in PBS/EtOH (70:30) to a final concentration of 100 μg/mL. Then 350 μL of the diluted compound solution (100 μg/mL) were added to the donor wells. The filter membrane was coated with PBL in dodecane (selected empirically as 4 μL volume of 20 μg/mL PBL in dodecane) and the acceptor wells were filled with 200 μL of PBS/EtOH (70:30). The acceptor filter plate was carefully put on the donor plate to form a sandwich (consisting of the aqueous donor with test compound on the bottom, lipid membrane in the middle and the aqueous acceptor on the top), which was left undisturbed for 18 h at 25 °C. After incubation, the donor and acceptor plates were separated carefully and the concentration of drug in the donor and acceptor wells was determined using the Varioskan Flash Multimode Reader (Thermo Scientific). Every sample was analyzed at ten wavelengths in four wells and in at least three

independent runs. P_e was calculated using the following expression:

$P_e = -\ln [1 - C_A(t)/C_{equilibrium}]/[A \times (1/V_D + 1/V_A) \times t]$

$C_{equilibrium} = [C_D(t) \times V_D + C_A(t) \times V_A]/(V_D + V_A)$

Where P_e is permeability in the unit of cm/s. A is effective filter area and t is the permeation time. V_D is the volume of donor well and V_A is the volume of acceptor well. $C_A(t)$ is the compound concentration in acceptor well at time t, and $C_D(t)$ is the compound concentration in donor well at time t. Results are given as the mean ± SD. In the experiment, 11 quality control drugs of known BBB permeability were included to validate the analysis set. A plot of the experimental data versus literature values gave a strong linear correlation, $P_e(exp.) = 0.9163 \times P_e(bibl.) - 0.2247$ ($R^2 = 0.9558$). From this equation and taking into account the limit established by Di et al.[43] for BBB permeation, we determined that compounds with P_e values above 3.44×10^{-6} cm/s could cross the BBB.

Acknowledgments

This work was supported in part by the Chinese National Natural Science Foundation (20872099), the Research Fund for the Doctoral Program of Higher Education (20110181110079) and the National Science and Technology Major Project on "Key New Drug Creation and Manufacturing Program"(2013ZX09301304-002).

References and notes

1. Salloway, S.; Mintzer, J.; Weiner, M. F.; Cummings, J. L. *Alzheimer's Dementia* **2008**, *4*, 65.
2. Hamilton, G.; Evans, K. L.; MacIntyre, D. J.; Deary, I. J.; Dominiczak, A.; Smith, B. H.; Morris, A. D.; Porteous, D. J.; Thomson, P. A. *Neurosci. Lett.* **2012**, *510*, 6.
3. Schelterns, P.; Feldman, H. *Lancet Neurol.* **2003**, *2*, 539.
4. Huang, L.; Lu, C.; Sun, Y.; Mao, F.; Luo, Z.; Su, T.; Jiang, H.; Shan, W.; Li, X. *J. Med. Chem.* **2012**, *55*, 8483.
5. Sharma, A. K.; Pavlova, S. T.; Kim, J.; Finkelstein, D.; Hawco, N. J.; Rath, N. P.; Kim, J.; Mirica, L. M. *J. Am. Chem. Soc.* **2012**, *134*, 6625.
6. Liu, Q.; Qiang, X. M.; Li, Y.; Sang, Z. P.; Li, Y. X.; Tan, Z. H.; Deng, Y. *Bioorg. Med. Chem.* **2015**, *23*, 911.

7. Huang, M.; Xie, S. S.; Jiang, N.; Lan, J. S.; Kong, L. Y.; Wang, X. B. *Bioorg. Med. Chem. Lett.* **2015**, *25*, 508.
8. Bonda, D. J.; Wang, X.; Perry, G.; Nunomura, A.; Tabaton, M.; Zhu, X.; Smith, M. A. *Neuropharmacology* **2010**, *59*, 290.
9. Braidy, N.; Poljak, A.; Marjo, C.; Rutlidge, H.; Rich, A.; Jayasena, T.; Inestrosa, N. C.; Sachdev, P. *Front. Aging Neurosci.* **2014**, *6*.
10. Yanovsky, I.; Finkin-Groner, E.; Zaikin, A.; Lerman, L.; Shalom, H.; Zeeli, S.; Weill, T.; Ginsburg, I.; Nudelman, A.; Weinstock, M. *J. Med. Chem.* **2012**, *55*, 10700.
11. Lee, S.; Zheng, X.; Krishnamoorthy, J.; Savelieff, M. G.; Park, H. M.; Brender, J. R.; Kim, J. H.; Derrick, J. S.; Kochi, A.; Lee, H. J. *J. Am. Chem. Soc.* **2013**, *136*, 299.
12. Modak, M. A.; Parab, P.; Ghaskadbi, S. S. *Diabetes/Metab. Res. Rev.* **2014**, *30*, 31.
13. Maynard, C. J.; Bush, A. I.; Masters, C. L.; Cappai, R.; Li, Q. X. *Int. J. Exp. Pathol.* **2005**, *86*, 147.
14. El-Faham, A.; Al Marhoon, Z.; Abdel-Megeed, A.; Khattab, S. N.; Bekhit, A. A.; Albericio, F. *Bioorg. Med. Chem. Lett.* **2015**, *25*, 70.
15. Patil, P. O.; Bari, S. B.; Firke, S. D.; Deshmukh, P. K.; Donda, S. T.; Patil, D. A. *Bioorg. Med. Chem. Lett.* **2013**, *21*, 2434.
16. Pisani, L.; Barletta, M.; Soto-Otero, R.; Nicolotti, O.; Mendez-Alvarez, E.; Catto, M.; Introcaso, A.; Stefanachi, A.; Cellamare, S.; Altomare, C. *J. Med. Chem.* **2013**, *56*, 2651.
17. Pisani, L.; Catto, M.; Leonetti, F.; Nicolotti, O.; Stefanachi, A.; Campagna, F.; Carotti, A. *Curr. Med. Chem.* **2011**, *18*, 4568.
18. Dias, K. S.; Jr, V. C. *Curr. Neuropharmacol.* **2014**, *12*, 239.
19. Agis-Torres, A.; Sölhuber, M.; Fernandez, M.; Sanchez-Montero, J. M. *Curr. Neuropharmacol.* **2014**, *12*, 2.
20. Prati, F.; Uliassi, E.; Bolognesi, M. L. *Med.chem.commun.* **2014**, *5*, 853.
21. Okombi, S.; Rival, D.; Bonnet, S.; Mariotte, A.-M.; Perrier, E.; Boumendjel, A. *J. Med. Chem.* **2006**, *49*, 329.
22. Maya, Y.; Ono, M.; Watanabe, H.; Haratake, M.; Saji, H.; Nakayama, M. *Bioconjugate Chem.* **2008**, *20*, 95.
23. Ono, M.; Maya, Y.; Haratake, M.; Ito, K.; Mori, H.; Nakayama, M. *Biochem. Biophys. Res.*

Commun. **2007**, *361*, 116.

24. Watanabe, H.; Ono, M.; Kimura, H.; Kagawa, S.; Nishii, R.; Fuchigami, T.; Haratake, M.; Nakayama, M.; Saji, H. *Bioorg. Med. Chem. Lett.* **2011**, *21*, 6519.
25. Geldenhuys, W. J.; Funk, M. O.; Van der Schyf, C. J.; Carroll, R. T. *Bioorg. Med. Chem. Lett.* **2012**, *22*, 1380.
26. Morales-Camilo, N.; Salas, C. O.; Sanhueza, C.; Espinosa-Bustos, C.; Sepúlveda-Boza, S.; Reyes-Parada, M.; Gonzalez-Nilo, F.; Caroli-Rezende, M.; Fierro, A. *Chem. Biol. Drug Des.* **2015**, *85*, 685.
27. Ono, M.; Yoshida, N.; Ishibashi, K.; Haratake, M.; Arano, Y.; Mori, H.; Nakayama, M. *J. Med. Chem.* **2005**, *48*, 7253.
28. Meguellati, A.; Ahmed-Belkacem, A.; Yi, W.; Haudecoeur, R.; Crouillère, M.; Brillet, R.; Pawlotsky, J. M.; Boumendjel, A.; Peuchmaur, M. *Eur. J. Med. Chem.* **2014**, *80c*, 579.
29. Zhang, M.; Xu, X. H.; Cui, Y.; Xie, L. G.; Kong, C. H. *Pest Manage. Sci.* **2012**, *68*, 1512.
30. Haudecoeur, R.; Ahmed-Belkacem, A.; Yi, W.; Fortuné, A.; Brillet, R.; Belle, C.; Nicolle, E.; Pallier, C.; Pawlotsky, J.-M.; Boumendjel, A. *J. Med. Chem.* **2011**, *54*, 5395.
31. Liu, B.; Zhang, M.; Xu, X. H.; Xie, L. G.; Chinese Patent CN 101914081 A, **2010**.
32. Lu, C.; Guo, Y.; Li, J.; Yao, M.; Liao, Q.; Xie, Z.; Li, X. *Bioorg. Med. Chem. Lett.* **2012**, *22*, 7683.
33. Buechi, G.; Weinreb, S. M. *J. Am. Chem. Soc.* **1971**, *93*, 746.
34. Manjulatha, K.; Srinivas, S.; Mulakayala, N.; Rambabu, D.; Prabhakar, M.; Arunasree, K. M.; Alvala, M.; Rao, M. V. B.; Pal, M. *Bioorg. Med. Chem. Lett.* **2012**, *22*, 6160.
35. Lee, C. Y.; Chew, E. H.; Go, M. L. *Eur. J. Med. Chem.* **2010**, *45*, 2957.
36. King, T. J.; Hastings, J. S.; Heller, H. G. *J. Chem. Soc., Perkin Trans.* **1975**, 1455.
37. Manuela, B.; Carlo, B.; Laura, B. M.; Andrea, C.; Carlo, M.; Vincenza, A. *Chembiochem* **2007**, *8*, 2152.
38. Sang, Z. P.; Qiang, X. M.; Li, Y.; Yuan, W.; Liu, Q.; Shi, Y. K.; Ang, W.; Luo, Y. F.; Tan, Z. H.; Deng, Y. *Eur. J. Med. Chem.* **2015**, *94*, 348.
39. Legoabe, L. J.; Petzer, A.; Petzer, J. P. *Bioorg. Chem.* **2012**, *45*, 1.
40. Novaroli, L.; Reist, M.; Favre, E.; Carotti, A.; Catto, M.; Carrupt, P. A. *Bioorg. Med. Chem.* **2005**, *13*, 6212.

41. Strydom, B.; Malan, S. F.; Castagnoli, N.; Bergh, J. J.; Petzer, J. P. *Bioorg. Med. Chem.* **2010**, *18*, 1018.

42. Dávalos, A.; Gómez-Cordovés, C.; Bartolomé, B. *J. Agric. Food Chem.* **2004**, *52*, 48.

43. Di, L.; Kerns, E. H.; Fan, K.; Mcconnell, O. J.; Carter, G. T. *Eur. J. Med. Chem.* **2003**, *38*, 223.

44. Sang, Z. P.; Li, Y.; Qiang, X. M.; Xiao, G. Y.; Liu, Q.; Tan, Z. H.; Deng, Y. *Bioorg. Med. Chem.* **2015**, *23*, 668.

45. Michela, R.; Elena, S.; Manuela, B.; Andrea, C.; Luisa, C.; Nicoleta, P.; David W, M.; Andrea, T.; Maria L, B.; Anna, M. *J. Med. Chem.* **2008**, *51*, 4381.

46. Li, R. S.; Wang, X. B.; Hu, X. J.; Kong, L. Y. *Bioorg. Med. Chem. Lett.* **2013**, *23*, 2636.

47. Geng, J.; Li, M.; Wu, L.; Ren, J.; Qu, X. *J. Med. Chem.* **2012**, *55*, 9146.

48. Nicoletta, D.; Adriana, B.; Rossella, F.; Luca Proietti, M.; Matilde, Y. E.; Francesco, O.; Stefano, A. *J. Med. Chem.* **2011**, *54*, 2155.

49. Sang, Z. P.; Qiang, X. M.; Li, Y.; Wu, B.; Zhang, H.; Zhao, M. G.; Deng, Y. *Chem. Biol. Drug Des.* **2015**, *86*, 1168.

50. He, Y.; Yao, P. F.; Chen, S. B.; Huang, Z. H.; Huang, S. L.; Tan, J. H.; Li, D.; Gu, L. Q.; Huang, Z. S. *Eur. J. Med. Chem.* **2013**, *63*, 299.

Graphical Abstract